Representation of nonrectangular features for exposure estimation and proximity effect correction in electron-beam lithography

S.-Y. Lee,[a] F. Hu, and J. Ji
Department of Electrical and Computer Engineering, Auburn University, Auburn, Alabama 36849

(Received 10 June 2004; accepted 4 October 2004; published 10 December 2004)

In most proximity effect correction schemes, circuit features are assumed to be rectangular. However, there are many circuit patterns which contain nonrectangular shapes of features such as circles, circular arcs, polygons, etc. In this article, efficient ways to handle such features for exposure estimation required in proximity effect correction are proposed. A hierarchical approach, where a nonrectangular feature is partitioned into *correction shapes* first, and then each correction shape may be further decomposed into *exposure shapes* if necessary, is taken in order to develop efficient and generally applicable schemes. Specifically, for exposure estimation, four schemes (*direct, slicing, hybrid,* and *coordinate transformation* methods) are described, of which performances have been analyzed through an extensive simulation. © *2004 American Vacuum Society.* [DOI: 10.1116/1.1824058]

I. INTRODUCTION

Estimation of exposure contributions from circuit features to a point or region is an important computational procedure not only for simulation of exposure distribution in the resist but also for proximity effect correction in e-beam lithography. How shapes of circuit features are represented has a direct effect on computation speed and accuracy. For rectangular features, efficient methods for exposure estimation exist. For *global* exposure contributions which are from "far-away" rectangular features, most methods adopt some kind of approximation where only the area (not shape) of a feature is taken into account since the spatial variation of point spread function (PSF) is minimal when the distance from the point of exposure (the origin of PSF) is large.[1,2] This approximation allows fast calculation of global exposure contributions without introducing significant errors. Such an approximation method cannot be employed for calculating *local* exposure contributions from "nearby" features since the PSF varies rapidly in the region close to its origin. An exact pixel-by-pixel convolution method is impractical because of its prohibitively long computation time required due to the large number of pixels usually contained in a circuit pattern. An exact method which adopts the concept of cumulative distribution function (CDF) in computing the local exposure for *rectangular* features and is several orders of magnitude faster than the point-by-point (spatial or frequency domain convolution) method, was developed in the PYRAMID project.[1]

However, it is not trivial to handle nonrectangular shapes of features such as circles, circular arcs, general polygons, etc. in exposure estimation and proximity effect correction. Note that the CDF approach is not directly applicable to such nonrectangular features since it is designed strictly for rectangular features.

In this article, a hierarchical approach to estimating exposure contributions from nonrectangular features and efficient implementations of the approach for typical nonrectangular shapes, i.e., circles, rotated rectangles, and polygons, are described along with simulation results. In this approach, a nonrectangular feature is decomposed through a two-step hierarchical procedure, i.e., first into *correction shapes* and then *exposure shapes* if necessary. This makes the implementations systematic and flexible, leading to accurate and fast local exposure calculation. Four methods (*direct, slicing, hybrid,* and *coordinate transformation* methods) for computing exposure contributions from exposure shapes are described, and their performances are compared in terms of accuracy and computation speed via simulation.

II. EXPOSURE ESTIMATION

Most proximity effection correction schemes require exposure (electron energy deposited at a pixel) to be estimated at certain control (or "critical") points.[3,4] Exposure distribution in a circuit pattern is obtained by the space-invariant linear convolution between an image corresponding to the circuit pattern (dose distribution within the pattern) and the point spread function (PSF) describing the energy deposition profile in the resist when a point is exposed. Due to the large number of features, exposure estimation is usually very time-consuming and, therefore, is to be implemented efficiently. A two-level approach was proposed, which decomposes exposure into two components, local and global exposures.[1] In estimation of the global exposure which is due to distant features, a coarse-grain convolution is employed. For estimating the local exposure which is due to features close to a control point, an efficient and exact scheme, referred to as CDF method, was developed for rectangular features. While the CDF method is orders of magnitude faster than a pixel-by-pixel convolution, most of the computational load in proximity effect correction is incurred still in local exposure estimation. Hence, in this article, only the local exposure estimation is addressed.

[a]Electronic mail: leesooy@eng.auburn.edu

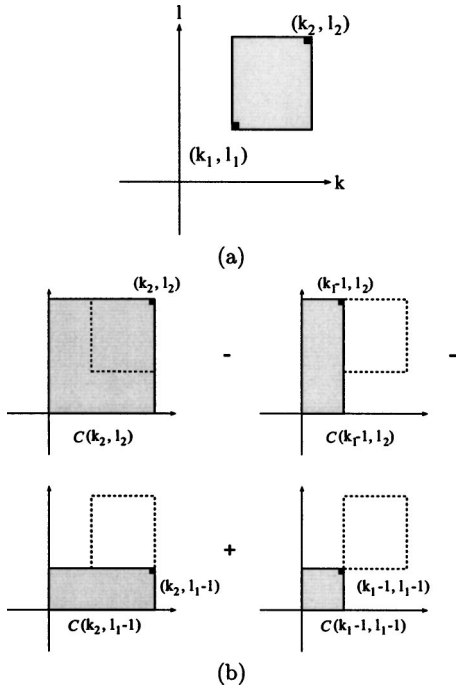

FIG. 1. Illustration of the CDF convolution method: (a) a rectangle whose convolution value (Conv) at the origin is to be calculated and (b) a graphical interpretation of $\mathcal{C}(k_2,l_2)-\mathcal{C}(k_1-1,l_2)-\mathcal{C}(k_2,l_1-1)+\mathcal{C}(k_1-1,l_1-1)=\text{Conv}$.

A. CDF method

A look-up table, or CDF table, is precomputed, which contains exposure contribution to the origin from various sizes of rectangular features where one (e.g., lower-left) vertex of each rectangle is at the origin. Exploiting the space-invariant *linearity* of integration (summation), the exact calculation of exposure contribution from a rectangular feature, which is assumed to be assigned a single dose, to a control point (which is at a certain distance from the feature) can be completed by two subtractions and one addition using the CDF table (following four table look-ups) in most cases. The concept of this CDF convolution method is illustrated in Fig. 1, where $C(k,l)$, which is an entry of the CDF table, denotes the exposure contribution (convolution) to the origin (0,0) from a rectangle of which two (opposite) vertices are at (0,0) and (k,l). Note that a point-by-point direct convolution would take $O(kl)$ time, compared to $O(1)$ time required by the CDF method. For more detail, refer to Ref. 1.

B. Nonrectangular features

Though most of the proximity effect correction schemes developed so far assume that circuit features are rectangles, there are many circuit patterns which include nonrectangular features such as circles, polygons, etc.[5–7] For example, a photonic band gap (PBG) structure may consist of a 2D array of circular features; a horizontal or vertical bus line may turn slanted, generating a segment of trapezoidal shape; some device circuit patterns may include shapes like hexagon, octagon, trapezoid, etc. Nonrectangular shapes of circuit features considered in this article are circle, rectangles with any orientation, and polygons.

The CDF method for rectangles is not directly applicable to most of nonrectangular features due to the difficulty in generating look-up (CDF) tables. Nevertheless, as will be described later, it is possible to build look-up tables for circles and right triangles, i.e., CDFC (CDF for circles) and CDFT (CDF for triangles) tables (note that the CDF table refers to the look-up table for rectangles). By using these three look-up tables, exposure contribution from any nonrectangular feature can be calculated without using a pixel-by-pixel convolution.

III. HIERARCHICAL APPROACH

A hierarchical approach to handling nonrectangular features is taken in order to make exposure estimation not only efficient but also applicable to various shapes. A nonrectangular circuit feature is first partitioned, if necessary, into *correction shapes* where a single dose is to be determined for each correction shape, i.e., dose modification (spatial control of dose within each circuit feature) is assumed for proximity effect correction where correction shape is the "unit of correction." Note that a circuit feature itself can be a correction shape, e.g., a circle may be assigned a single dose.

When exposure contribution from a shape can be computed by looking up only one of the three tables (CDF, CDFC, and CDFT tables), the shape is referred to as a "basic shape." There are three basic shapes that are supported in the current implementation, i.e., rectangle, circle, and right triangle. When a correction shape is not a basic shape, it is further decomposed into *exposure shapes* where each exposure shape is a basic shape. In other words, correction shape is for dose control to correct proximity effect and exposure shape is for facilitating exposure estimation required in proximity effect correction. This two-level approach makes exposure estimation and proximity effect correction more general and efficient for nonrectangular features.

IV. CORRECTION SHAPES

In certain circuit patterns, a nonrectangular feature itself may be a correction shape. That is, a single dose for the entire feature is to be determined. However, in most cases, a feature is partitioned into regions (referred to as correction shapes in this article) where a dose is determined for each region, in order to achieve sufficient spatial control of dose within each feature.[8] Dose determination for each region is based on the exposure estimate at the corresponding control point.

A. Circles

When a circle does not need to be corrected or just needs to be roughly corrected, the circle itself can be a correction shape. That is, a single dose is determined for the circle, i.e., no spatial dose control within the circle. When it is necessary to control dose spatially within a circle, the circle may be

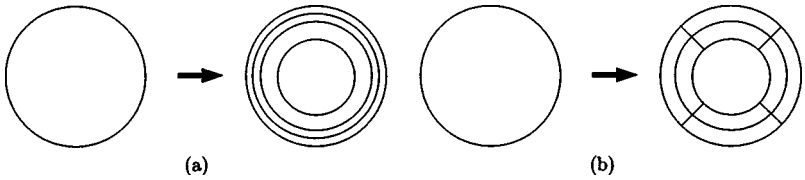

FIG. 2. Correction shapes for a circle feature: (a) ring, a circle is divided into concentric rings and a center circle where a dose is to be determined for each ring and the center circle and (b) arc, each ring may be further divided into arcs for an improved spatial control of dose.

partitioned into concentric rings (and a center circle) and a dose is determined for each ring. In such a case, the correction shape of ring is used as shown in Fig. 2(a). When exposure varies significantly around a circle, the correction shape of ring may not provide sufficient dose control within the circle for proximity effect correction. Then, each ring may be further divided into arcs as illustrated in Fig. 2(b), where each ring is partitioned into 4 equal arcs. Hence, for a circle, three correction shapes are considered, i.e., circle, ring, and circular arc, where circular arc is not a basic shape.

B. Polygons

Note that a rotated rectangle can be included in the category of (convex) polygon and, therefore, it is not considered separately. It should be clear that a concave polygon can be decomposed into a set of convex polygons. A polygonal feature is partitioned into a set of correction shapes, a center region, edge regions, and corner regions, where the center region is a smaller similar polygon, as illustrated in Fig. 3. A separate dose is to be determined for each region. Note that a corner region is a parallelogram and an edge region is a trapezoid. That is, all correction shapes generated from a polygon (where the number of sides is greater than 4) are not of basic shape in general. Therefore, each of them needs to be further partitioned into a set of basic exposure shapes.

In the proposed hierarchical approach, correction shapes that can be generated from partitioning nonrectangular features are circle, ring, circular arc, polygon, and rectangle.

V. EXPOSURE SHAPES

Each correction shape is associated with a dose and, given a critical point, exposure contribution from the correction shape to the critical point is to be computed. Four methods have been considered for calculating exposure contribution from a nonrectangular correction shape, i.e., *direct, slicing, hybrid*, and *coordinate transformation* methods.

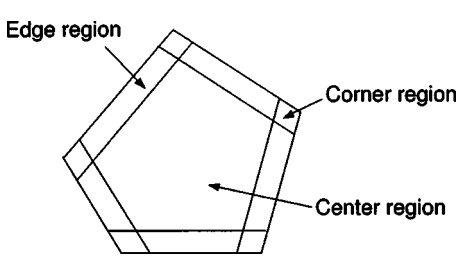

FIG. 3. Correction shapes generated from a polygon where the corner region is a parallelogram, the edge region is a trapezoid, and the center region is a similar polygon.

A. Direct method

For a nonrectangular correction shape of circle, ring, or right triangle, i.e., a basic shape, its exposure contribution can be computed directly from one of the look-up tables.

1. Circle and ring

A CDFC table which is computed *a priori* to store exposure contributions from circles with the size and distance from the critical point varied is utilzed. The CDFC table is a two-dimensional (2D) array parameterized by the radius of a circle and the distance from the center of the circle to a point at which exposure is to be computed, i.e., a critical point. To find exposure contribution from a circle to a critical point, one just needs to read the corresponding entry in the CDFC table. This table can also be utilized for computing exposure contribution from a ring, which may be derived as the difference between two circles with different radii. That is, two table look-ups and a subtraction are needed for a ring. Compared to the slicing method (refer to Sec. V B), the direct method can reduce computation time for exposure estimation greatly though it requires an additional table (CDFC table) and is only applicable to certain shapes.

2. Right triangle

A CDFT table stores exposure contributions from right triangles with the size and distance varied where a right triangle is oriented such that its two sides, joining at the right-angle vertex, are either horizontal or vertical. The CDFT table is a 4D array where two dimensions are used to specify the coordinates of the right-angle vertex of a triangle in the local coordinate system whose origin is at the critical point, and the other two dimensions for its base and height. Given the coordinates of the right-angle vertex of a (right) triangle, there can be various sizes of triangles, each of which can have four different orientations. Varying size and different orientations are represented by allowing both *positive* and *negative* bases and heights. One drawback of using the CDFT table is that the memory requirement is large (compared to other tables) due to the high dimensionality of the table.

A rectangle can be represented by a linear combination of other rectangles, which is the fundamental reason why the CDF table method is so efficient. However, that is not possible for a circle or right triangle, e.g., a right triangle cannot be represented by a linear combination of other right triangles. This makes the CDFC and especially CDFT tables larger compared to the CDF table.

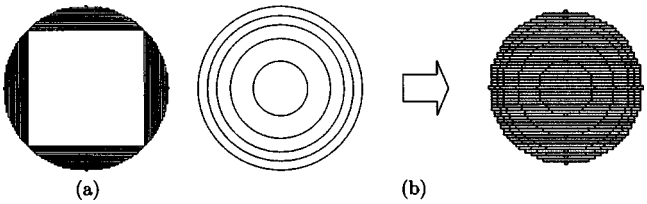

FIG. 4. Slicing method: (a) a correction shape of circle is partitioned into exposure shapes of rectangles (a square and slices) and (b) correction shapes of rings are partitioned into exposure shapes of rectangles.

B. Slicing method

Any (nonrectangular) shape may be decomposed into thin slices (exposure shapes) such that each slice is a rectangle. Then, only the CDF table is needed for exposure estimation. That is, this method is generally applicable to any shape, but computationally intensive due to the large number of slices generated. The main issue is how to minimize the number of rectangles resulted from the partitioning (note that the number of rectangles determines computation time required for exposure estimation in this method). A partitioning scheme which minimizes the number of resulting rectangles without introducing any error is illustrated for the correction shape of circle in Fig. 4(a) and for the correction shape of ring in Fig. 4(b). A circle is divided into the largest square inscribed and four remaining parts that are sliced into one-pixel high or wide rectangles.

C. Hybrid method

In order to minimize the computation time required in the slicing method by reducing the number of exposure shapes generated from a correction shape, a nonrectangular correction shape may be decomposed into a set of rectangles and right triangles. For example, a polygon may be decomposed into a set of rectangles and right triangles as illustrated in Fig. 5.

In minimizing the number of exposure shapes especially when a correction shape is thin, the concept of "negative triangle" may be adopted, as illustrated in Fig. 6 where there are 1 rectangle, 4 triangles, and 2 negative triangles generated from a rotated rectangle. That is, the middle parallelogram is represented by the bounding rectangle and two negative triangles. Exposure contribution from a negative triangle is considered to be negative. That is, the exposure contribution from the parallelogram is derived by subtracting the exposure contributions of the two negative triangles from that of the bounding rectangle. Without using the negative triangles, a larger number of exposure shapes would be generated from the parallelogram.

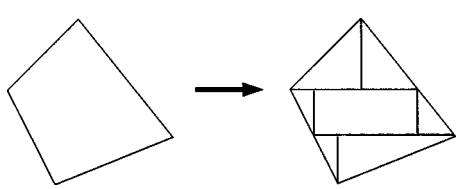

FIG. 5. Hybrid method: a correction shape of polygon is decomposed into exposure shapes of rectangles and right triangles.

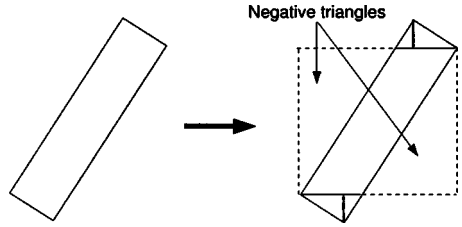

FIG. 6. In the hybrid method, a portion of correction shape may be represented by a rectangle and *negative* right triangles.

D. Coordinate transformation

A correction shape of rotated rectangle may be generated from a slanted bus line, a polygon, etc. Given a rotated rectangle and a critical point at which exposure contribution from the rotated rectangle is to be estimated, the local coordinates (x,y) centered at the critical point may be rotated such that the rectangle is not slanted (i.e., horizontally or vertically oriented) in the new coordinates (x',y') as illustrated in Fig. 7. Then, the CDF table (for rectangles) can be used to derive the exposure contribution. This method can avoid paritioning the correction shape of a rotated rectangle at the expense of coordinate transformation.

VI. PERFORMANCE ANALYSIS

A. Exposure estimation

In Table I, the direct and slicing methods are compared for the correction shape of circle. At each of the points along a slanted radial line passing through the center of the circle, exposure contribution from the circle is estimated by the direct method ($\text{Exposure}_{\text{direct}}$) and is compared to that ($\text{Exposure}_{\text{slicing}}$) by the slicing method. Taking the slicing method as a reference, percentage exposure "error" is defined to be $|\text{Exposure}_{\text{direct}}-\text{Exposure}_{\text{slicing}}|/\text{Exposure}_{\text{slicing}} \times 100$ (note that it may be considered as percentage exposure *difference* since it is not really an error). In Table I, the maxi-

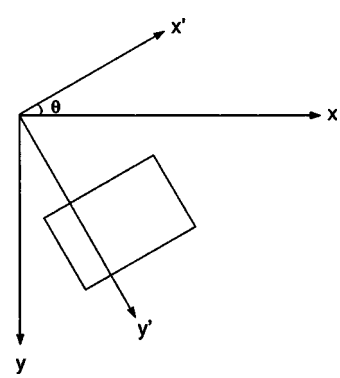

FIG. 7. Coordinate transformation from (x,y) to (x',y') for a rotated rectangle. Note that the sides of the rectangle are parallel with the new axes (x',y') so that the CDF table can be used.

TABLE I. Percentage exposure error and exposure estimation time (100 000 iterations) by the direct method for a circle (correction shape) where pixel size is 2 nm [the substrate of 1000 nm PMMA on Si (50 keV)]. A Sun Sparc V9 (450 MHz) was used.

	Percentage error (%)		Estimation time (s)	
Radius (pixel)	Maximum	Average	Direct	Slicing
25	1.940	0.205	0.19	1.56
50	1.240	0.115	0.19	2.95
75	1.002	0.075	0.19	4.86
100	1.425	0.093	0.20	6.73
125	0.830	0.054	0.19	8.44
150	0.900	0.057	0.19	10.14

mum and average percentage exposure errors are shown for various sizes of circle. The percentage errors are averaged over all points considered. It can be seen that the error is very small, especially for large circles. Also, in the table, exposure estimation time is compared between the slicing and direct methods. It is clear that the direct method can reduce exposure estimation time greatly. The larger the circles, the larger the reduction.

In Table II, the hybrid and slicing methods are compared for the correction shape of arc [refer to Fig. 2(b) where the ring width is 1/5 of the radius]. Note that the direct method is not applicable to this case. Percentage exposure errors ($|\text{Exposure}_{\text{hybrid}} - \text{Exposure}_{\text{slicing}}|/\text{Exposure}_{\text{slicing}} \times 100$) are averaged over all points along the radial line. While errors are still small (the average error not greater than 2%), they are relatively larger compared to the cases where the correction shape is circle (refer to Table I). It is mainly due to the mismatch between each arc and its representation approximated by rectangles and right triangles. Also, it is seen that, except for small features, the hybrid scheme is significantly faster than the slicing scheme as expected.

For the correction shape of rotated rectangle, the slicing and hybrid methods are compared to the coordinate transformation method which is considered to be "accurate." That is, the reference for error (in Table III) is the coordinate transformation method, not the slicing method. A rectangle of size 20×15 in pixel (where the pixel size is 5 nm), rotated by the angle θ, is used for performance analysis. The hybrid method uses the CDFT table of which size grows fast as the maximum size of right triangle to be covered increases. The size of the memory available on a workstation limits the size of the CDFT table and accordingly the size of exposure shape. Exposures at points along the line perpendicular to the width of the rectangle are estimated for analyzing percentage exposure error and estimation time. The results are provided in Table III.

TABLE II. Percentage exposure error and exposure estimation time (100 000 iterations) by the hybrid method for a circle with the correction shape of arc where the pixel size is 2 nm [the substrate of 1000 nm PMMA on Si (50 keV)]. A Sun Sparc V9 450 MHz was used.

	Percentage error (%)		Estimation time (s)	
Radius (pixel)	Maximum	Average	Hybrid	Slicing
25	1.17	0.31	17.2	6.1
50	2.28	1.56	16.4	12.9
75	4.13	2.03	18.2	20.7
100	1.90	1.24	18.6	29.0
125	2.28	1.11	20.5	37.7

TABLE III. Angle dependency of percentage exposure error (compared to the coordinate transform method) and exposure estimation time (1 000 000 iterations) for a rotated rectangle. The pixel size is 5 nm [the substrate of 1000 nm PMMA on Si (50 keV)]. A Sun Sparc V9 450 MHz was used.

		Percentage error (%)				Estimation time (s)		
		Slicing		Hybrid		Coord. trans.	Slicing	Hybrid
Angle (θ°)	$\tan(\theta)$	Max	Ave	Max	Ave			
75.964	4	8.82	5.87	18.10	13.74	12.18	12.88	5.48
63.435	2	11.29	3.00	21.65	2.87	11.99	14.15	6.36
45.000	1	10.36	5.62	11.10	6.22	7.93	13.89	4.35
36.870	0.75	8.20	4.27	4.20	3.11	7.99	12.87	4.20
26.565	0.5	7.13	3.43	10.13	5.89	8.12	12.75	6.62
14.036	0.25	6.12	1.79	29.94	13.50	8.11	11.75	5.91

In Table III, it is seen that the percentage exposure error is relatively large compared to that for circles. One of the reasons is that a (slanted) straight edge is harder to approximate by discrete pixels than a curved one. Also, the size of the rotated rectangle used is so small that the percentage error is "magnified." However, the error would be much smaller for larger rectangles. As expected, the hybrid method achieves the shortest exposure estimation time since the number of exposure shapes generated by the hybrid method is least (among the three methods), especially compared to the slicing method which usually generates a large number of thin rectangles. While the coordinate transformation method requires only one table look-up, the computation required for coordinate transformation involves evaluation of trigonometric functions which are much more time-consuming than

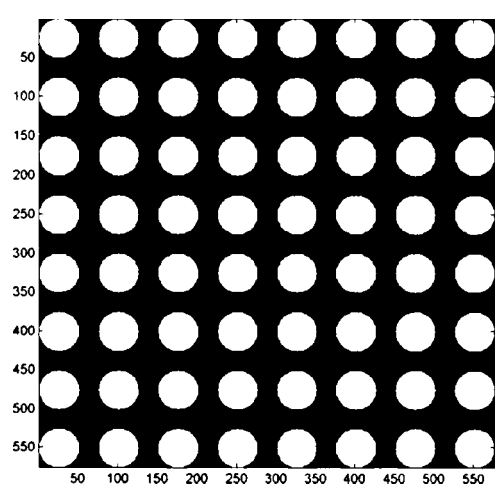

FIG. 8. Test circuit pattern of a 2D array of circles where the radius of circle is 50 nm and the gap between adjacent circles is 50 nm. The pixel size is 2 nm.

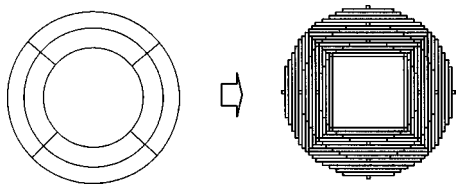

FIG. 9. Each arc (correction shape) is decomposed into slices (exposure shape).

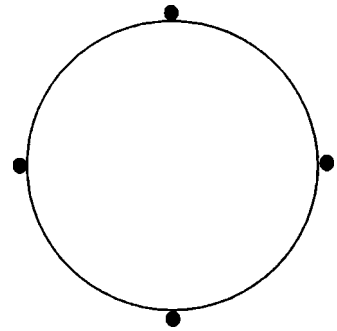

FIG. 10. Four critical points are set up for each circle in the test circuit pattern.

simple arithmetic operations. The coordinate transformation method turns out to be still faster than the slicing method on average, but slower than the hybrid method.

B. Correction

A simple circuit pattern which consists of identical circles arranged in a square array, shown in Fig. 8, is used to analyze correction performance. Two correction shapes are considered: ring and arc.

Ring: Each circle is decomposed into concentric rings and a dose is to be determined for each ring such that CD (critical dimension) error is minimized. Two methods for exposure estimation are considered: slicing and direct methods. In the slicing method, each ring is partitioned into thin rectangles for exposure estimation [refer to Fig. 4(b)]. As discussed in Sec. V A, in the direct method, exposure contribution from each ring is computed by two CDFC table look-ups and a subtraction.

Arc: Each circle is decomposed into rings and a center circle, and then each ring into 4 arcs [refer to Fig. 2(b)]. A dose is determined for each arc and the center circle, to minimize the CD error. In order to minimize the number of exposure shapes, the arcs and center circle are sliced in both horizontal and vertical directions as illustrated in Fig. 9. Since the direct method for exposure estimation is not applicable in this case, only the slicing and hybrid methods are compared.

On the boundaries of each circle, 4 critical points are set up (refer to Fig. 10), at which CD errors are evaluated by computing the difference between the ideal and actual (blurred) boundaries. The size of circle and gap between adjacent circles are varied. In Table IV, correction results are summarized, where CD error, "slope" (edge exposure contrast), and correction time are provided. In terms of correction accuracy, the correction shape of arc leads to a smaller CD error and a higher contrast than the correction shape of

TABLE IV. Correction accuracy and time for circuit patterns which consist of circles arranged in a square array (refer to Fig. 8) corrected for the substrate of 1000 nm PMMA on Si (50 keV). For the exposure shapes of rectangle, ring, and hybrid, the slicing, direct and hybrid methods are used, respectively. A Sun Sparc V9 450 MHz was used.

Circuit		Shape		Accuracy				Speed	
Radius (nm)	Gap (nm)	Correction shape	Exposure shape	CD error (nm) Max	CD error (nm) Ave	Contrast ($\mu C/cm^2$) Min	Contrast ($\mu C/cm^2$) Ave	Time (s)/ iteration	Number of iterations
50	50	Ring	Rectangle	0.767	0.183	1.907	1.982	21.19	22
			Ring	0.767	0.183	1.907	1.982	0.54	22
		Arc	Rectangle	0.110	0.097	1.850	1.924	7.35	20
			Hybrid	0.038	0.016	1.861	1.936	26.65	20
	200	Ring	Rectangle	0.110	0.081	2.298	2.309	22.05	14
			Ring	0.110	0.081	2.298	2.309	0.55	14
		Arcs	Rectangle	0.110	0.081	2.298	2.309	7.16	23
			Hybrid	0.009	0.009	2.266	2.277	26.86	23
100	100	Ring	Rectangle	0.444	0.109	1.774	1.810	51.38	16
			Ring	0.444	0.109	1.774	1.810	0.57	16
		Arc	Rectangle	0.110	0.085	1.780	1.816	15.70	17
			Hybrid	0.178	0.159	1.806	1.842	29.26	17
	200	Ring	Rectangle	0.201	0.093	1.877	1.896	31.37	9
			Ring	0.201	0.093	1.877	1.896	0.38	9
		Arcs	Rectangle	0.089	0.082	1.894	1.914	10.35	18
			Hybrid	0.158	0.152	1.923	1.942	17.70	18

ring as expected. The improvement by using arcs is larger for a denser circuit pattern. Also, it is seen that there is no difference in correction accuracy between the exposure shapes of rectangle (slicing) and ring (direct) when the correction shape is ring. The (average) difference in exposures computed by the slicing and direct methods is very small as shown in Table I, which resulted in the same correction of this particular circuit pattern by the two methods. Using the exposure shape of ring leads to a much faster correction than using the exposure shape of rectangle when the correction shape is ring. This is mainly because the slicing method generates a larger number of exposure shapes (regions) from each ring while a ring itself is an exposure shape, i.e., a basic shape, in the direct method. When the correction shape is arc, correction time is shorter for the slicing method than for the hybrid method. However, for larger circles, it is expected that the hybrid method would perform better in terms of correction speed.

VII. SUMMARY

In this study, the issue of handling nonrectangular features in proximity effect correction is addressed by developing methods of computing exposure contributions from such features "exactly" and analyzing their performance via simulation. In the proposed approach, a nonrectangular feature is partitioned into *correction shapes* for dose control, and each correction shape is decomposed into *exposure shapes* if it is not a *basic* shape (rectangle, circle, ring, and right triangle). Four methods have been considered for exposure calculation. The direct method is efficient, but applicable only to the basic shapes of features. While the slicing method can be used for any arbitrary shape of feature, it is usually more time-consuming than other methods, due to the large number of slices generated from a nonrectangular feature. The hybrid method which decomposes a nonrectangular shape into a set of rectangles and right triangles is able to reduce the exposure estimation time significantly compared to the slicing method. However, it requires an additional look-up table for right triangles, which is much larger than the one for rectangles. The coordinate transformation method can be effective in computing exposure contribution from a rotated rectangle. All these methods are exact in the sense that they are equivalent to a pixel-by-pixel convolution given a basic exposure shape. The simulation results indicate that the methods described in this paper will enable accurate correction of nonrectangular features without approximation in exposure estimation.

ACKNOWLEDGMENT

This work was supported in part by a research grant (DMI-0214624) from NSF.

[1]S.-Y. Lee and B. D. Cook, IEEE Trans. Semicond. Manuf. **11**, 108 (1998).
[2]M. Osawa, K. Takahashi, M. Sato, and H. Arimoto, J. Vac. Sci. Technol. B **19**, 2483 (2001).
[3]U. Hofmann, C. Kalus, A. Rosenbusch, R. Jonckheere, and A. Hourd, in *Proceedings of SPIE Conference on E-Beam, X-Ray, EUV, and Ion-Beam Sub-Micrometer Lithographies for Manufacturing VI*, Vol. 2723, pp. 150–158, March 1996.
[4]M. Peckerar, R. Bass, and K. Rhee, J. Vac. Sci. Technol. B **18**, 3143 (2000).
[5]O. Painter, R. Lee, A Scherer, A, Yariv, J. O'Brien, P. Dapkus, and I. Kim, Science **284**, 1819 (1999).
[6]J. Moosburger, T. Happ, M. Kamp, and A. Forchel, J. Vac. Sci. Technol. B **18**, 3501 (2000).
[7]M. H. Park, Y. K. Hong, S. H. Gee, and D. W. Erickson, Appl. Phys. Lett. **83**, 329 (2003).
[8]S.-Y. Lee and D. He, Microelectron. Eng. **69**, 47 (2003).